Magnetic domain configurations of epitaxial chromium dioxide (CrO_2) nanostructures

Xiaojing Zou[a] and Gang Xiao
Department of Physics, Brown University, Providence, Rhode Island 02912, USA

(Received 19 July 2007; accepted 24 August 2007; published online 12 September 2007)

Magnetic domain structures of submicrometric epitaxial CrO_2 fabricated using selective-area growth technique were studied by magnetic force microscopy. In-plane, lamellar domain structure with fragmented walls aligned along the magnetic easy axis direction is observed, indicating the existence of a large magnetocrystalline anisotropy. A classical model for ferromagnetic materials with a uniaxial anisotropy was used to explain this domain configuration. Estimates of the domain wall energy density and exchange stiffness constant for CrO_2 were obtained. © *2007 American Institute of Physics*. [DOI: 10.1063/1.2784946]

Spintronics is an emerging area, where the electron spin (together with the charge) plays an active role in storing and transferring information.[1] In this area, half-metallic ferromagnets have been extensively investigated for realizing spin-dependent devices with high magnetoresistance. These materials have a band gap in the minority spin density of states near the Fermi level and therefore exhibit a 100% spin polarization. Among these materials, chromium dioxide (CrO_2) is one of the few experimentally proven half metals and possesses the largest spin polarization so far reported.[2–4]

On the other hand, the study of magnetic nanostructures has also been a very active research field. One of the reasons for this is that applications in ultrahigh-density magnetic recording require the element dimensions to be reduced down to the nanometer scale. Also, interesting changes in the magnetic behavior of nanostructures are expected as the overall size approaches some critical length.[5] Hence, the study of the properties of nanosized half-metallic ferromagnets is a very promising field. In this letter, we describe the fabrication of epitaxial CrO_2 nanostructures. We have also investigated the remanent magnetic domain configuration of these elements by using magnetic force microscopy.

The fabrication of CrO_2 structures at the nanometer scale is a challenging task. So far, there has been no single reliable recipe available. This is due to the metastable nature of CrO_2, which can easily decompose into Cr_2O_3. Prior to this work, various methods have been attempted to pattern small CrO_2 structures, including wet etching, reactive ion etching (RIE),[6] and focused ion beam milling.[7] In all these methods, CrO_2 thin films are deposited and then etched to make small patterns. These processing methods inevitably cause degradation of the quality of CrO_2 after the etching step. Another approach for creating patterned chromium dioxide elements is the selective-area growth technique.[8] In this method, patterned SiO_2 is first deposited onto a TiO_2 substrate and then CrO_2 is grown selectively on the areas not covered by SiO_2 because CrO_2 has zero sticking coefficient on SiO_2 substrates. This avoids the need to pattern the CrO_2 film after deposition and, hence, subsequent degradation of the film. In this work, we have extended the selective-area growth technique to enable the fabrication of high quality single crystal CrO_2 nanostructures with individual feature size smaller than 80 nm.

The experimental process is shown schematically in Fig. 1(a). First, a layer of silicon dioxide was deposited onto the (100) TiO_2 substrate and then a 350 nm thick polymethylmethacrylate (PMMA) was spin coated onto the SiO_2 film. After baking at 185 °C for 30 min, a thin layer of chromium was deposited by electron beam evaporation and patterns were then defined by e-beam lithography in a LEO 20 kV scanning electron microscope (SEM). After removal of the chromium layer in a Cr etchant solution, the developed PMMA was used as the etching mask for the RIE of the underlying SiO_2 layer, which is carried out in a CHF_3 atmosphere. The introduction of CHF_3 allows anisotropic etching for perpendicular sidewalls and high aspect ratio features. After the RIE of SiO_2, the remaining PMMA was removed using acetone and the sample was carefully cleaned in isopropanol and de-ionized water before the CrO_2 deposition. Chromium dioxide was grown by chemical vapor deposition (CVD) using CrO_3 as the precursor. Details of the CVD process have been reported previously.[9] The deposition time is controlled strictly so as to achieve an intended thickness.

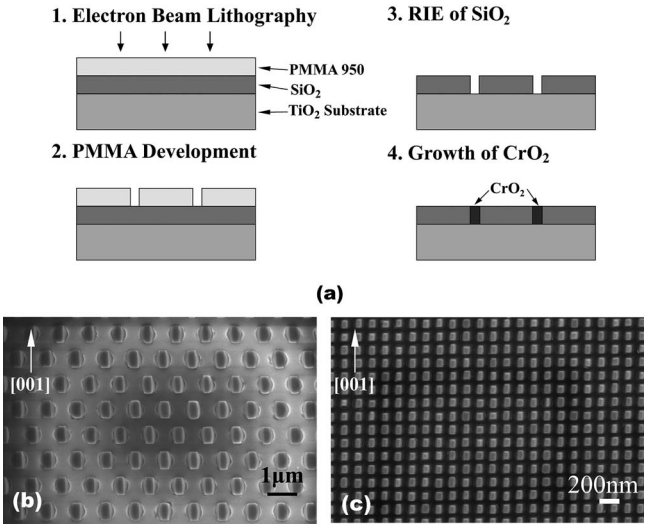

FIG. 1. (a) Schematic diagrams of the process used to fabricate nanosized chromium dioxide structures, and SEM images of (b) a hexagonal lattice of 300 nm sized CrO_2 dots and (c) a square lattice of 80 nm sized CrO_2 dots.

[a]Electronic mail: xiaojing_zou@brown.edu

The SEM images of CrO_2 nanodot arrays in hexagon and square lattices are shown in Figs. 1(b) and 1(c). As can be seen, all the dots are distinct and well separated. The epitaxial (100) TiO_2 substrate ensures that the grown CrO_2 nanodots also have (100) texture and can be regarded as nanosized extensions of the substrate. Furthermore, it was observed that, first, the CrO_2 covers the bottom of the e-beam defined circular holes and then beyond a certain thickness, the nanodots start to become rectangular shaped (viewed from the top) with long side parallel to the *c* axis ([001] direction). This indicates that the lateral growth rate in CrO_2 nanodots is anisotropic and a maximum at an intermediate angle between the [010] and [001] directions. More specifically, in our case, this is the diagonal direction of the rectangle. It is believed that the anisotropy in surface binding energy leads to the rectangular shape[10] but the detailed kinetic process is not very clear.

Chromium dioxide nanostructures with nanowire and ring shapes have also been fabricated on the same substrate to ensure identical magnetic and structural properties. The sample was first saturated along the easy axis ([001]) direction by applying a magnetic field of 2 kOe and then imaged in the remanent state using magnetic force microscopy (MFM). The MFM images were obtained with a Digital Instruments nanoscope IIIa scanning probe microscope in tapping mode with the scanning tip magnetized along the *z* direction (perpendicular to the sample surface). Figures 2(a) and 2(b) are MFM images of CrO_2 nanowires of various widths aligned along the [001] and [010] directions. In Fig. 2(a), all the domains are aligned in plane along the magnetic easy axis. It is clear that the magnetic stray field signals at the element ends are very strong even for the 100 nm width, with no out-of-plane field observed in the rest of the wire. This indicates a high quality single domain structure with a fully in-plane magnetization. For the wires in Fig. 2(b), lamellar domain structures with fragmented walls, aligned mainly along the easy axis direction, are observed. Each wire is either magnetized parallel or antiparallel to the [001] direction, across its width, leading to an alternating contrast in the MFM image. A similar result has been reported recently for epitaxial CrO_2 wire with 2 μm width.[11] This domain configuration implies that a strong magnetocrystalline anisotropy exists in the [001] direction for these epitaxial chromium dioxide elements. The formation of multiple domains can be attributed to the competition between magnetostatic energy and domain wall energy, which will be discussed in detail later.

The magnetic image of an epitaxial CrO_2 ring in the remanent state is displayed in Fig. 2(c). Unlike the vortex and onion states found in other ferromagnetic rings, the epitaxial CrO_2 ring displays a much more complicated domain structure.[12] As can be seen, two large parallel domains are formed in the upper and lower parts of the ring and separated by many relatively small antiparallel domains in between. This configuration is consistent, again, with the existence of a strong uniaxial anisotropy along the easy axis direction, as found in Fig. 2(b).

The strong magnetocrystalline anisotropy is more obvious in the MFM image of the Y-shaped structure shown in Fig. 2(d). The shape anisotropy induced in this structure is almost negligible in comparison to the uniaxial anisotropy, given that every domain is aligned along the magnetic easy axis.

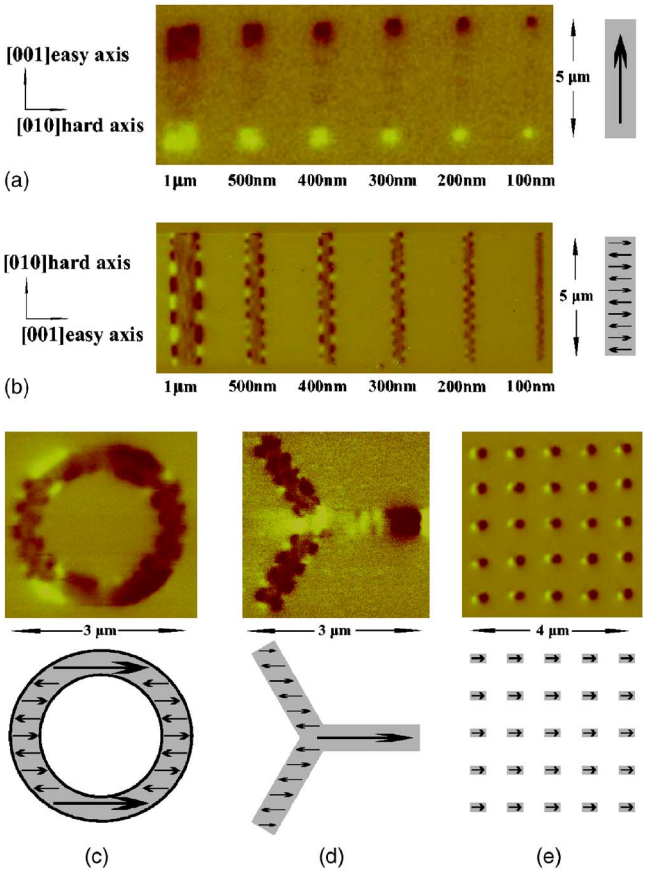

FIG. 2. (Color online) MFM images of submicron-sized CrO_2 wires with different widths aligned (a) along the [001] direction and (b) along the [010] direction. The thickness of the wires is around 100 nm. (c) A CrO_2 ring with 300 nm width, (d) a Y-shaped pattern with one arm aligned along the magnetic easy axis, and (e) a portion of a square lattice of 250 nm sized nanodots. All the images were obtained at remanence after a saturation in a magnetic field applied along the easy axis direction. The schematic pictures shown nearby are the most probable domain configurations.

Epitaxial CrO_2 nanodots with a diameter of 250 nm also show a single domain configuration along the [001] direction, as displayed in Fig. 2(e). These dots exhibit a strong signal-to-noise ratio and a strong magnetocrystalline anisotropy which dominates the shape anisotropy contribution, which suggest that epitaxial CrO_2 nanodots are a potential candidate for high-density state storage media.[13]

We also found that the domain configurations for different wires aligned along the hard axis direction were closely related to the wire aspect ratio. As indicated in Fig. 3(a), the domain width *d* can be calculated approximately by dividing the length of the wire by the number of domains, while the domain length *L* is roughly the width of the wire. The plot in Fig. 3(b) shows that a linear relationship exists between the domain width and length. This result is consistent with the model for a uniaxial sheet of magnetic material with lamellar domain formation. By minimizing the total energy density, including magnetostatic and domain wall energy, the equilibrium wall spacing for small thickness *t* can be written as[14]

$$d = L\sqrt{\frac{\sigma_d}{1.7\mu_0 M_s^2 t}}, \tag{1}$$

where σ_d is the domain wall energy density, and M_s is the saturation magnetization, which has a value of 475 emu/cm^3 at room temperature. The domain wall energy density can be

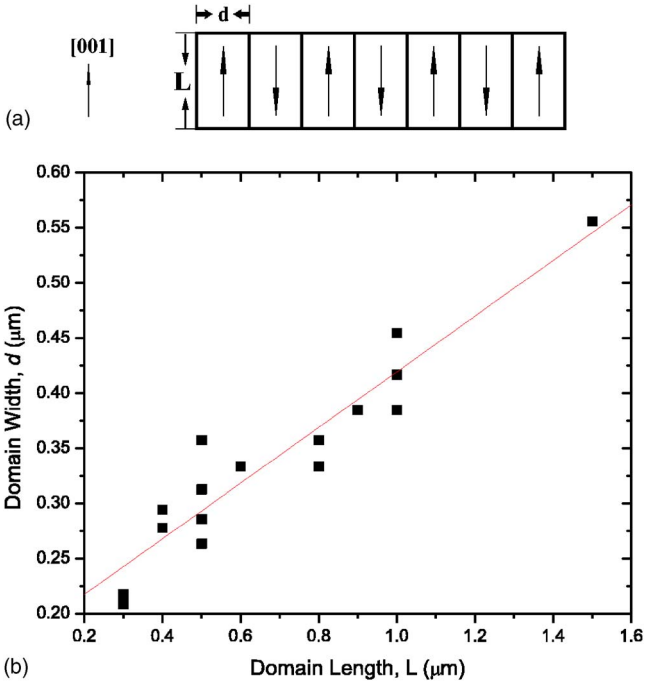

FIG. 3. (Color online) (a) Schematic drawing including the definitions of domain length L and width d. (b) Domain width plotted vs domain length for several typical CrO_2 lines aligned along the [010] axis. The width is calculated by dividing the length of the wire by the number of observed domains. The line is the best fit to the data according to theoretical predictions.

estimated to be 0.25 erg/cm^2 for a thickness $t=100$ nm.

On the other hand, for this uniaxial case with an antiparallel domain configuration, the domain wall energy density can be approximated as

$$\sigma_d \sim \sqrt{AK_u}, \tag{2}$$

where K_u is the uniaxial anisotropy constant, which gives a value of around 1.43×10^5 erg/cm^3 for an epitaxial CrO_2 thin film with $t=100$ nm.[15] Thus, the exchange stiffness constant A is estimated to be 4.37×10^{-7} erg/cm, which is very closed to the value of 4.6×10^{-7} erg/cm calculated from the Curie temperature of CrO_2.

In summary, we have presented a method to fabricate submicrometric single crystal chromium dioxide structures. The use of the selective-area growth technique for patterning small elements avoids the degradation of the CrO_2 film caused by the commonly applied etching process. The anisotropy induced by the lattice mismatch can be directly inferred from the rectangular shape of the single crystal CrO_2 nanodots, which have their long side parallel to the c axis. This can be attributed to the difference in the lattice constant mismatch between CrO_2 and the TiO_2 substrate for the b and c axes. We have studied the domain configuration of several CrO_2 patterns grown epitaxially on TiO_2 (100) including nanodots, nanowires, and ring structures using MFM. The in-plane, stripelike, domain structures with domain walls aligned mainly along the [001] direction indicate a strong magnetocrystalline anisotropy, which makes the shape anisotropy contribution almost negligible. We have also found that all the domains tend to have a similar aspect ratio. This can be understood with a classical model for uniaxial magnetic films. Our results show that the epitaxial CrO_2 nanostructures have the potential to be applicable in spintronic devices.

This work was supported in part by the NSF under Grant No. DMR-0605966. We also gratefully acknowledge partial support from JHU MRSEC (NSF, DMR-0520491). G.X. wishes to thank Dr. Hai Sang for collaboration on characterization of half metals under the support of the National Natural Science Foundation of China under Grant No. 10128409.

[1] G. A. Prinz, Science **282**, 1660 (1998).
[2] Y. Ji, G. J. Strijkers, F. Y. Yang, C. L. Chien, J. M. Byers, A. Anguelouch, G. Xiao, and A. Gupta, Phys. Rev. Lett. **86**, 5585 (2001).
[3] R. J. Soulen Jr., J. M. Byers, M. S. Osofsky, B. Nadgorny, T. Ambrose, S. F. Cheng, P. R. Broussard, C. T. Tanaka, J. Nowak, J. S. Moodera, A. Barry, and J. M. D. Coey, Science **282**, 85 (1998).
[4] J. S. Parker, S. M. Watts, P. G. Ivanov, and P. Xiong, Phys. Rev. Lett. **88**, 196601 (2002).
[5] S. D. Bader, Rev. Mod. Phys. **78**, 1 (2006).
[6] Q. Zhang, Y. Li, A. V. Nurmikko, G. X. Miao, G. Xiao, and A. Gupta, J. Appl. Phys. **96**, 7527 (2004).
[7] L. Yuan, Y. Ovchenkov, A. Sokolov, C.-S. Yang, B. Doubin, and S. H. Liou, J. Appl. Phys. **93**, 6850 (2003).
[8] A. Gupta, X. W. Li, S. Guha, and G. Xiao, Appl. Phys. Lett. **75**, 2996 (1999).
[9] X. W. Li, A. Gupta, and G. Xiao, Appl. Phys. Lett. **75**, 713 (1999).
[10] J. J. Gilman, *The Art and Science of Growing Crystals* (Wiley, New York, 1963), p. 37.
[11] C. Konig, M. Fonin, M. Laufenberg, A. Biehler, W. Buhrer, M. Klaui, U. Rudiger, and G. Guntherodt, Phys. Rev. B **75**, 144428 (2007).
[12] X. Y. Liu, D. Mazumdar, B. D. Schrag, W. Shen, and G. Xiao, Phys. Rev. B **70**, 014407 (2004).
[13] C. A. Ross, H. T. Smith, T. Savas, M. Schattenburg, M. Farhoud, M. Hwang, M. Walsh, M. C. Abraham, and R. J. Ram, J. Vac. Sci. Technol. B **17**, 3168 (1999).
[14] R. C. O'Handley, *Modern Magnetic Materials: Principles and Applications* (Wiley, New York, 2004), p. 298.
[15] G. Miao, G. Xiao, and A. Gupta, Phys. Rev. B **71**, 094418 (2005).